


## Direct Measurements of Surface Strain-Mediated Lateral Interactions between Adsorbates in Colloidal Heteroepitaxy

Manodeep Mondal<sup>1,\*</sup> and Rajesh Ganapathy<sup>2,3</sup>

<sup>1</sup>*Chemistry and Physics of Materials Unit, Jawaharlal Nehru Centre for Advanced Scientific Research, Jakkur, Bangalore—560064, India*

<sup>2</sup>*International Centre for Materials Science, Jawaharlal Nehru Centre for Advanced Scientific Research, Jakkur, Bangalore—560064, India*

<sup>3</sup>*School of Advanced Materials (SAMat), Jawaharlal Nehru Centre for Advanced Scientific Research, Jakkur, Bangalore—560064, India*

 (Received 25 February 2022; revised 10 May 2022; accepted 5 July 2022; published 17 August 2022)

Surface strain can alter the dynamics of adsorbates, and often, the adsorbates themselves induce and interact via their surface strain fields. In epitaxy, such strain-mediated effects get further compounded when a misfit strain exists due to lattice mismatch between the growing film and substrate. Here, we carry out particle-resolved imaging of heteroepitaxial growth of multilayer colloidal films where the particles interact via a short-range attraction. Surprisingly, although the misfit strain relaxed systematically with film thickness, the adcolloid diffusivity was nonmonotonic. We show that this nonmonotonicity stems from the competition between the spatial extent of self-induced in-layer strain and the short interaction range. Importantly, we provide direct evidence for long-ranged strain-mediated interactions between adsorbates and show that it alters the growing film's morphology.

DOI: [10.1103/PhysRevLett.129.088003](https://doi.org/10.1103/PhysRevLett.129.088003)

Epitaxial growth is typically far from equilibrium. Thus, the island shape and number density and the three-dimensional (3D) film morphology are determined not by thermodynamics but by the kinetic barriers adsorbed particles experience for intra- and interlayer diffusion and attaching to other adparticles and islands [1–3]. Atomic epitaxy studies find that strain due to a lattice mismatch between the growing film and the substrate, i.e., heteroepitaxy, can strongly influence these kinetic barriers [4,5]. For compressive misfits ( $\epsilon < 0$ ), adatoms experience a less corrugated surface than the homoepitaxy case ( $\epsilon = 0$ ), and correspondingly the diffusion barrier is also smaller, while for tensile misfits ( $\epsilon > 0$ ), since adatoms sit deeper in the hollow sites, the barrier is larger due to long-ranged interactions with buried surface layers [3,6]. Here,  $\epsilon = [(\sigma_s - \sigma_f)/\sigma_f]$  is the misfit strain and  $\sigma_f$  is the film lattice constant and  $\sigma_s$  the substrate's. With continued particle deposition as the film thickness increases and the misfit strain is relaxed, the diffusion barrier becomes layer-dependent [7]. Besides the misfit strain, the very presence of adatoms can locally distort the underlying layer, especially for  $\epsilon > 0$ , and distant adatoms can interact laterally through their self-induced surface strain fields [8,9]. Atomic heteroepitaxy experiments, however, cannot yet measure strain fields beneath adatoms. Instead, these studies show that mean-field island growth laws, where strain effects are ignored, are violated [10], and this is considered indirect proof for their existence [11–13]. Surface strain effects can potentially be probed directly

in epitaxy with colloids, which are often considered “big” atoms [14,15]. Indeed, colloids obey the same homoepitaxial growth laws as atoms [16], and their epitaxy is also simpler [17–21]. In atomic epitaxy, electronic and elastic effects contribute to kinetic barriers [22], and being difficult to disentangle simulations findings can differ depending on how these effects are accounted for [4,23]. In colloidal heteroepitaxy, only elastic interactions matter. Given that an early theoretical study anticipated elastic effects to play a crucial role in surface physics due to their longer range over electronic ones [24], probing their role in colloidal epitaxy would be ideal.

Nontrivial surface strain-mediated effects can arise in colloidal heteroepitaxy due to the shorter interparticle interaction range in comparison to atoms. Interactions between colloids often span only a fraction of their size, and can even be sticky. Thus, the kinetic barriers here are due to real energy barriers and path length-dependent pseudobarriers [16,25,26]. Thus, from a self-assembly standpoint, mimicking the rich self-organized growth seen in atomic heteroepitaxy [27–29] with these larger building blocks first requires unraveling how the short interaction range alters surface strain effects.

Here, we experimentally study how a tensile misfit strain alters diffusion barriers and, consequently, the 3D film morphology during epitaxy with colloids interacting via a short-range depletion attraction [30]. We found that the adcolloid diffusion barrier is layer-dependent and, surprisingly, also nonmonotonic with film thickness—a feature

we show is exclusive to systems with short-range attraction. Importantly, we provide the first real-space evidence for strain-mediated long-range lateral interactions between adcolloids and show that it results in a violation of mean-field island growth laws.

In our study, we used charge-stabilized micron-sized silica colloids (diameter  $0.89 \mu\text{m}$ ) suspended in a fluorescent refractive index-matched mixture. A nonadsorbing polymer, sodium carboxymethyl cellulose (radius of gyration  $R_g \approx 33 \text{ nm}$ ), was used as the depletant to induce a short-range attraction between the particles and also between the particles and the substrate (see Supplemental Material [31]). We determined  $\sigma_f$  by letting the colloids crystallize on a featureless substrate. Next, the particles were sedimented on soft-lithographically patterned substrates with (100) symmetry, and we varied  $\sigma_s$  to access a range of  $\varepsilon$  spanning from 1% to 5.5% (see Supplemental Material, Figs. S1, S2, and S3 [31]) [26,42]. For the highest values of  $\varepsilon$  studied, particles occupying adjacent sites on the substrate are separated by a distance comparable to the range of the depletion interaction. The particle deposition flux  $F$ , and the strength of depletion attraction  $U$  were kept constant in all our experiments (Fig. S4 [31]).

Figure 1(a) shows the film morphology for four  $\varepsilon$  values 72 hrs after the onset of particle deposition. The particles are colored according to the layer number (see color bar) (Fig. S5 [31]). Like in atomic heteroepitaxy, with  $\varepsilon$  we observed a transition from layer-by-layer growth to the formation of 3D mounds [28,43]. Since  $F$  and  $U$  are fixed, this change in film morphology is only due to how the kinetic barriers for adcolloid diffusion and island attachment get dressed by the strain. For  $\varepsilon \geq 5.5\%$ , islands tended to dewet from the substrate and adopt a hexagonal symmetry [circled region in Fig. 1(a)]. Here, therefore, we restricted our attention to  $\varepsilon = 4.5\%$  and compared it with  $\varepsilon = 1\%$ , which is close to the homoepitaxy limit.

In atomic and also DNA-coated nanoparticle epitaxy, where the interactions are long-ranged, film growth is pseudomorphic—in registry with the substrate—up to a  $\varepsilon$ -dependent threshold height beyond which it becomes energetically favorable to relieve the strain, usually through the formation of misfit dislocations [44,45]. Further, these defects in atomic systems locally alter diffusion barriers and thereby promote or inhibit island nucleation [27]. In our system, however, forming dislocations is prohibitively energy-expensive due to the short range of the interaction [46], and it is unclear how strain relief occurs as film thickness increases. As a first step, we quantified the particle strain  $\varepsilon_p = [(\sigma_s - \sigma_p)/\sigma_p]$  [47], and then the average in-layer strain,  $\varepsilon_{\text{layer}} = \langle \varepsilon_p \rangle$  with film thickness [Fig. 1(b)]. Here,  $\sigma_p$  is the separation between a pair of nearest-neighbor (NN) particles in a given layer, and the  $\langle \rangle$  denote an average over all such pairs. Since island nucleation can locally alter  $\varepsilon_p$  in the underlying layer, we measured  $\varepsilon_{\text{layer}}$  at a layer coverage,  $\Theta = \Theta_{\text{Onset}}$ , which is

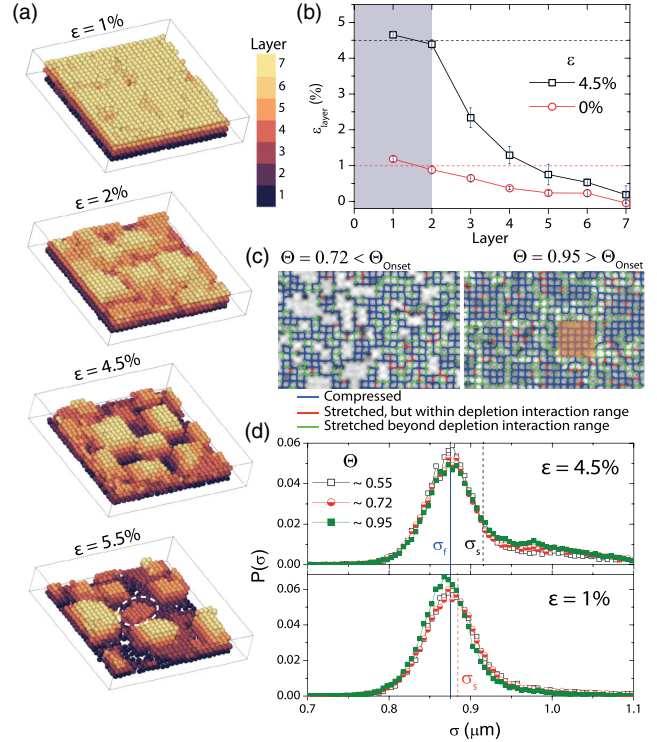


FIG. 1. (a) Film morphology for different misfit strain,  $\varepsilon$ , values with particle color representing the layer number (see color bar). For  $\varepsilon \geq 5.5\%$ , islands tended to dewet from the substrate and form hexagonal domains (circled region). (b) Average in-layer strain,  $\varepsilon_{\text{layer}}$ , with film thickness.  $\varepsilon_{\text{layer}}$  for each layer was measured at a coverage  $\Theta = \Theta_{\text{Onset}}$ , i.e., when island nucleation initiated in the layer above. The shaded region denotes pseudomorphic growth. (c) Nearest-neighbor bonds, colored according to legend, for  $\Theta$  below (left panel) and above (right panel)  $\Theta_{\text{Onset}}$  for  $\varepsilon = 4.5\%$ . (d) Bond-length distribution,  $P(\sigma)$ , for square-coordinated particles for  $\varepsilon = 4.5\%$  and  $\varepsilon = 1\%$  at various  $\Theta$ . The solid and dashed lines represent the equilibrium ( $\sigma_f$ ) and substrate lattice constant ( $\sigma_s$ ), respectively.

the coverage when island nucleation on top had just set in (see Supplemental Material and Fig. S6 [31]). For  $\varepsilon = 1\%$  (dashed red line), interparticle bonds are minimally stretched, and  $\varepsilon_{\text{layer}}$  (circles) falls gradually to zero. For  $\varepsilon = 4.5\%$ , however,  $\varepsilon_{\text{layer}}$  (squares) hovers around the imposed strain (dashed black line) for the first two layers (pseudomorphic growth) and then falls rapidly to zero.

The first and second layer film was pseudomorphic with the substrate only in an average sense; the individual bond lengths in these layers showed significant distortions. The left and right panels of Fig. 1(c) show the instantaneous snapshot of bonds in the first layer that are stretched or compressed with respect to  $\sigma_s$  for  $\Theta$  below and above  $\Theta_{\text{Onset}}$ , respectively (Video S1 [31]). Although many bonds are stretched beyond the range of depletion interactions, a previous study on a similar system found that entropy-driven thermal fluctuations of particles can lead to a nearly threefold increase in their effective interaction range [47].

Interestingly, for  $\Theta < \Theta_{\text{Onset}}$ , stretched bonds are not just localized to the island perimeter, where the coordination is low, but are present even in the island interior (Video S1 [31]). We gleaned further insights through the bond-length distribution  $P(\sigma)$  in the first layer for different  $\Theta$  for both values of  $\varepsilon$  [Fig. 1(d)]. For  $\varepsilon = 1\%$  (bottom panel), the peak of  $P(\sigma)$  is centered around  $\sigma_s$  (dashed red line) only for low to moderate coverages, while for  $\Theta > \Theta_{\text{Onset}}$ , the peak shifts to  $\sigma_f$  (solid line) due to island nucleation on top. This indicates that the wetting layer weakly adheres to the substrate. For  $\varepsilon = 4.5\%$ , for all  $\Theta$ , the peak of  $P(\sigma)$  is centered not at  $\sigma_s$  (dashed red line) but at  $\sigma_f$ , and importantly shows a long tail for  $\sigma > \sigma_s$ . Also, as the peak height of  $P(\sigma)$  with  $\Theta$ , the tail develops a clear shoulder. This is because when significant island nucleation has occurred on the first layer [ $\Theta > \Theta_{\text{Onset}}$ , right panel in Fig. 1(c)], compressed bonds are localized below these islands (see orange shaded region) while stretched ones are relegated to the regions below the island perimeter (see Supplemental Material and Fig. S7 [31]). Since the size of nucleating islands is small, perimeter bonds increase at the expense of interior ones. Thus, in-layer strain is partially relieved by local dewetting, and importantly, unlike in atomic systems [48], pseudomorphic growth is coverage-dependent in the epitaxy of particles with short-range attraction.

Because of strain relaxation, the amplitude of particle position fluctuations decreased in each subsequent layer (see Supplemental Material, Fig. S8 and Video S2 [31]), and we expected adcolloid diffusion barriers to show a layer dependence [26,49], especially for  $\varepsilon = 4.5\%$ . Also, just as islands distort bonds in the underlying layer, so can single adcolloids, which may influence their dynamics. Figure 2(a) shows the layer-dependent adcolloid diffusivity,  $D$ , for the two misfits (Fig. S9 [31]). As expected, for  $\varepsilon = 1\%$  (circles),  $D$  remains nearly constant within experimental uncertainty. Surprisingly,  $D$  for  $\varepsilon = 4.5\%$  (squares) is nonmonotonic with a minimum in the second layer.

To understand this observation, we quantified the local in-layer strain field due to an adcolloid above. For each layer, Fig. 2(b) shows  $\varepsilon_p$  for the first, second, and third NN particles for an adcolloid in the hollow site (Fig. S10 [31]). We diagrammatically represent this in Fig. 2(c), where the grids are bonds and the nodes are the particles. The grid colors represent the experimentally calculated  $\varepsilon_p$  (see color bar). The adcolloid on the first layer draws the four 1st NN particles that make the hollow site close by [colored red in Fig. 2(c-i)] and thus  $\varepsilon_p$  [triangles in Fig. 2(b)] is smaller than the imposed strain of 4.5% [dashed line in Fig. 2(b)] (Video S3 [31]). Consequently, the bonds between the 1st–2nd NN particles are considerably weakened, if not broken, because  $\varepsilon_p \approx 6\%$ , which is beyond the depletion interaction range (dark blue in Fig. 2(c-i); see color bar), while those between the 2nd–3rd NN particles remain intact [ $\varepsilon_p \approx \varepsilon = 4.5\%$ ; Fig. 2(b)]. However, the adcolloid and

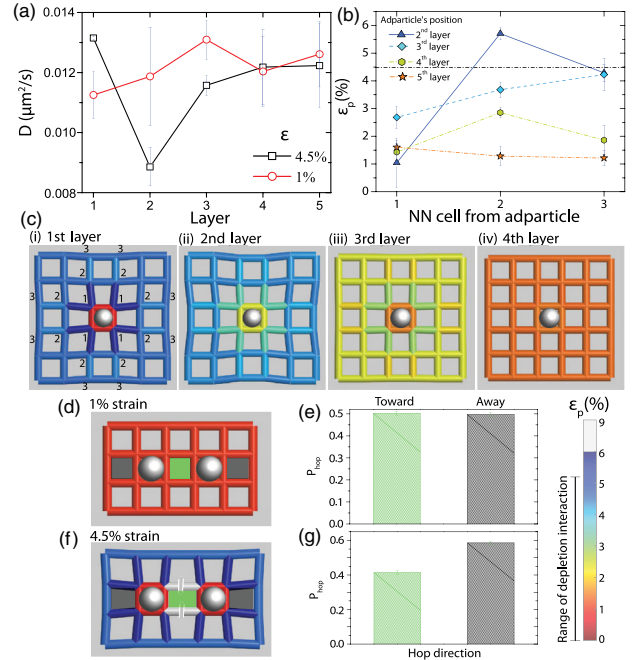


FIG. 2. (a) Adcolloid diffusivity,  $D$ , on each layer for  $\varepsilon = 4.5\%$  and  $\varepsilon = 1\%$ . (b) Particle strain,  $\varepsilon_p$ , in the layer beneath the adcolloid for the 1st, 2nd, and 3rd nearest-neighbor (NN) particles for  $\varepsilon = 4.5\%$ .  $\varepsilon_p$  is measured when the adcolloid is at a hollow site and the symbols represent the layer in which the adcolloid resides. (c) Diagrammatic representation of (b). Here, the grid colors represent the experimentally measured  $\varepsilon_p$  (see color bar). Notice that the grid is maximally distorted from a square shape in the 2nd layer. The range of the adcolloid-induced strain field is largest here and results in a minimum in  $D$ . (d) and (f) show  $\varepsilon_p$  in the first layer, for a pair of adcolloids separated by  $\sigma_s$  above for  $\varepsilon = 4.5\%$  and  $\varepsilon = 1\%$ , respectively. (e) and (g) show the probability  $P_{\text{hop}}$  for adcolloids to make a hop toward or away from each other for  $\varepsilon = 4.5\%$  and  $\varepsilon = 1\%$ , respectively.

1st NN particle bonds are unstable as these particles are frustrated having dewetted from the substrate and broken in-layer neighbor bonds.  $D$  is thus large on the first layer [Fig. 2(a)].

In the second layer,  $\varepsilon_{\text{layer}}$  is smaller than in the first due to strain relaxation, but this influences  $D$  on this layer. Unlike in the first layer, even with an adcolloid above, in-layer 1st–2nd NN particle bonds are now intact; they are within the depletion interaction range [diamonds in Figs. 2(b) and 2(c-ii)]. Also, since the strain is not fully relaxed, second layer particles have room to rattle (Fig. S8 [31]). As the adcolloid attempts to hop from a hollow site, it drags the 1st NN particles along, which cascades to the 2nd and 3rd NN particles. The enhanced particle cooperativity accompanying a hop on the second layer significantly reduces  $D$ . Importantly, since low particle mobilities promote the nucleation of many small and disconnected islands, the small  $D$  on the second layer coincides with the transition from pseudomorphic growth to 3D island formation [ $\varepsilon = 4.5\%$ ; Fig. 1(a)]. For the third layer and beyond,



$\varepsilon_{\text{layer}}$  is further reduced [Fig. 1(b); Figs. 2(c-iii) and 2(c-iv)], and since particles in these layers do not have much rattle room (Fig. S8 [31]), they cannot be dragged along during a hop. An adcolloid hop now involves breaking two 1st NN bonds, and these particles are stable, unlike in the first layer, and thus,  $D$  increases again, albeit it is smaller than on the first. The competing effects of two length scales, the first set by the spatial extent of adcolloid-induced in-layer strain and the second by the short-range of the depletion interaction, result in the nonmonotonic evolution of  $D$  with film thickness.

We now considered if faraway adcolloids could interact laterally through their self-induced surface strain fields. We first identified adcolloid pairs on the first layer separated by  $2\sigma_s$ , which is almost 25 times the depletion interaction range. We then quantified the probability,  $P_{\text{hop}}$ , for particles to make a hop toward or away from each other from  $\approx 1500$  hops. We ensured these pairs were far from other adsorbates. On a strain-free layer, given the short attractive interaction range, particle hops toward and away should be equally likely, and this is indeed true for  $\varepsilon = 1\%$  [Figs. 2(d) and 2(e)]. Strikingly, for  $\varepsilon = 4.5\%$ , hops away are more likely than hops toward each other [Fig. 2(g)] (Video S4 [31]). This is because even as each adcolloid draws its 1st NN particles close by [Fig. 2(f)], for a hop toward the other adcolloid to be successful 1st NN bonds at the new site have to readily form and this is hampered by the short interaction range. To our knowledge, this observation constitutes the first real-space experimental evidence for surface strain-mediated lateral interactions between adsorbates in epitaxial growth.

We now expect surface strain-mediated effects to be more accentuated for adcolloid-island interactions. Indeed, atomic epitaxy studies find that nucleation of islands on a strained layer can lead to trench formation and denuded zones around them [50]. These zones can alter adparticle attachment probabilities and hence the island growth laws, and we attempted to measure them here directly. For a square island in the second layer, Figs. 3(a) and 3(b) show  $\varepsilon_p$  in the first layer over a region below the island and also around one of the island edges for the two  $\varepsilon$  values. As expected, for the smaller misfit,  $\varepsilon_p \approx \varepsilon = 1\%$  (see color bar), and is uninfluenced by the island above. However, for  $\varepsilon = 4.5\%$ , we observed a trench near the island perimeter with  $\varepsilon_p > 20\%$  (see color bar) since the island particles pull those in the layer below close by to maximize their coordination (Video S5 [31]).

We quantified the influence of trench or denuded zones on adcolloid-island interactions through the residence time,  $\tau_R$ , of adcolloids at hollow sites located at various distances,  $R$ , perpendicular to the island edge [see schematic in Fig. 3(c)]. The magnitude of  $\tau_R$  is proportional to the diffusion barrier. For  $\varepsilon = 1\%$ ,  $\tau_R$  is nearly constant for  $R/\sigma_s \geq 2$  since islands do not distort the underlying layer [Fig. 3(d)].  $\tau_R$  is large for  $R/\sigma_s = 1$  simply because the

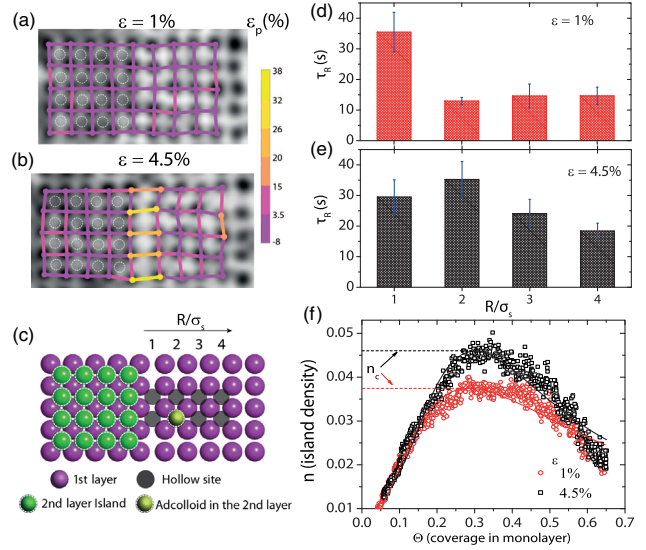


FIG. 3. (a) and (b) show an island on the first layer for  $\varepsilon = 4.5\%$  and  $\varepsilon = 1\%$ , respectively. The particles in the island are shown by dashed white circles. The part of the image containing the island also appears darker during imaging due to the presence of an additional layer of particles. The overlaid lines represent  $\varepsilon_p$  in the first layer (see color bar). (d) and (e) show the residence time  $\tau_R$  of adcolloids at hollow sites located at various distances  $R/\sigma_s$  from the island edge for  $\varepsilon = 1\%$  and  $\varepsilon = 4.5\%$ , respectively.  $\tau_R$  is the duration that an adparticle center lies inside a square box of size  $0.5\sigma_f$  centered at the hollow site [26]. See schematic shown in (c). (f) Island density  $n$  versus  $\Theta$  for the two misfits.

adcolloid is now also bonded to particles at the island edge. Most strikingly, for  $\varepsilon = 4.5\%$ ,  $\tau_R$  is a maximum for  $R/\sigma_s = 2$  and the strain field decreases gradually for larger values of  $R/\sigma_s$  [Fig. 3(e)]. Thus, the self-generated surface strain fields by islands and adparticles lead to an effective lateral long-ranged repulsion between them (Video S6 [31]).

The strain-mediated effective adcolloid-island repulsion should inhibit the growth of large islands. In epitaxy, the island number density  $n$  first increases as arriving particles nucleate new islands and then reaches a maximum,  $n_c$ —the saturation island density—as new adparticles diffuse and become part of existing islands [16,51]. With increasing coverage,  $n$  decreases due to islands coalescence. At fixed  $F$ , a large  $n_c$  indicates a tendency to form 3D islands, while a small  $n_c$  signifies a tendency for layer-by-layer growth. Mean-field island growth laws, which predict  $n_c \sim (F/D)^{1/3}$ , break down due to strain effects [52], but drawing this inference from atomic epitaxy experiments is plagued by difficulties in measuring  $D$  directly [53]. Figure 3(f) shows  $n$  versus  $\Theta$  on the first layer for  $\varepsilon = 1\%$  (circles) and  $\varepsilon = 4.5\%$  (squares) (see Supplemental Material and Fig. S11 [31]). Since  $F$  and  $U$  are constant (see Supplemental Material and Figs. S12, S4 [31]), a direct comparison of island growth for the two misfits is possible.

Although  $D_{\varepsilon=4.5\%} > D_{\varepsilon=1\%}$  on the first layer [Fig. 2(a)],  $n_c$  is larger for  $\varepsilon = 4.5\%$  indicating the breakdown of the island growth laws (see Supplemental Material and Fig. S13 [31]).

Collectively, our particle-resolved experiments have unraveled the rich interplay of short-ranged particle interactions and adsorbate-induced surface strain fields in colloidal heteroepitaxy. For misfit strains comparable to the attractive interaction range, even as the in-layer strain relaxes systematically with film thickness, the spatial extent of adcolloid-induced strain fields becomes nonmonotonic, and hence, so do adcolloid mobilities. Most importantly, adcolloid-adcolloid and adcolloid-island interactions get dressed by their self-induced strain fields, and the resulting effective long-range interactions, which are repulsive here, lead to a violation of island growth laws. While strain-mediated effects are known to be operative in atomic systems, experimental evidence for these is often indirect [8,11,22,54]. These effects, however, transcend length scales, and we directly measured them here in a model colloidal system. Our findings can shed light on many other surface processes, including catalysis [55] and heterogeneous nucleation [56].

M. M. thanks UGC-CSIR for a research fellowship. R. G. thanks DST-Nanomission (SR/NM/TP-25/2016) and DST SwarnaJayanthi fellowship (DST/SJF/PSA-03/2015-16) for financial support.

\*Corresponding author.

deep.manodeep10@gmail.com

- [1] Z. Zhang and M. G. Lagally, Atomistic processes in the early stages of thin-film growth, *Science* **276**, 377 (1997).
- [2] K. Bromann, H. Brune, H. Röder, and K. Kern, Interlayer Mass Transport in Homoepitaxial and Heteroepitaxial Metal Growth, *Phys. Rev. Lett.* **75**, 677 (1995).
- [3] M. Schroeder and D. E. Wolf, Diffusion on strained surfaces, *Surf. Sci.* **375**, 129 (1997).
- [4] H. Brune, K. Bromann, H. Röder, K. Kern, J. Jacobsen, P. Stoltze, K. Jacobsen, and J. Norskov, Effect of strain on surface diffusion and nucleation, *Phys. Rev. B* **52**, R14380 (1995).
- [5] C. Ratsch, Strain dependence for microscopic growth parameters for Ag on Ag (100), *Phys. Rev. B* **83**, 153406 (2011).
- [6] E. Penev, P. Kratzer, and M. Scheffler, Effect of strain on surface diffusion in semiconductor heteroepitaxy, *Phys. Rev. B* **64**, 085401 (2001).
- [7] A. Picone, M. Riva, G. Fratesi, A. Brambilla, G. Bussetti, M. Finazzi, L. Duò, and F. Ciccacci, Enhanced Atom Mobility on the Surface of a Metastable Film, *Phys. Rev. Lett.* **113**, 046102 (2014).
- [8] K. H. Lau and W. Kohn, Elastic interaction of two atoms adsorbed on a solid surface, *Surf. Sci.* **65**, 607 (1977).
- [9] I. Brihuega, Adatom-Adatom Interaction Mediated by an Underlying Surface Phase Transition, *Phys. Rev. Lett.* **98**, 156102 (2007).
- [10] K. Binder, Theory of first-order phase transitions, *Rep. Prog. Phys.* **50**, 783 (1987).
- [11] A. Bogicevic, S. Ovesson, P. Hyldgaard, B. I. Lundqvist, H. Brune, and D. R. Jennison, Nature, Strength, and Consequences of Indirect Adsorbate Interactions on Metals, *Phys. Rev. Lett.* **85**, 1910 (2000).
- [12] S. Ovesson, Mean-Field Nucleation Theory with Nonlocal Interactions, *Phys. Rev. Lett.* **88**, 116102 (2002).
- [13] R. Grima, J. DeGraffenreid, and J. A. Venables, Mean-field theory of nucleation and growth on strained surfaces, *Phys. Rev. B* **76**, 233405 (2007).
- [14] W. Poon, Colloids as big atoms, *Science* **304**, 830 (2004).
- [15] D. M. Herlach, T. Palberg, I. Klassen, S. Klein, and R. Kobold, Overview: Experimental studies of crystal nucleation: Metals and colloids, *J. Chem. Phys.* **145**, 211703 (2016).
- [16] R. Ganapathy, M. R. Buckley, S. J. Gerbode, and I. Cohen, Direct measurements of island growth and step-edge barriers in colloidal epitaxy, *Science* **327**, 445 (2010).
- [17] A. van Blaaderen, R. Ruel, and P. Wiltzius, Template-directed colloidal crystallization, *Nature (London)* **385**, 321 (1997).
- [18] J. P. Hoogenboom, A. K. van Langen-Suurling, J. Romijn, and A. van Blaaderen, Hard-Sphere Crystals with hcp and Non-Close-Packed Structure Grown by Colloidal Epitaxy, *Phys. Rev. Lett.* **90**, 138301 (2003).
- [19] A. van Blaaderen, J. P. Hoogenboom, D. L. J. Vossen, A. Yethiraj, A. van der Horst, K. Visscher, and M. Dogterom, Colloidal epitaxy: Playing with the boundary conditions of colloidal crystallization, *Faraday Discuss.* **123**, 107 (2003).
- [20] J. P. Hoogenboom, A. K. van Langen-Suurling, J. Romijn, and A. van Blaaderen, Epitaxial growth of a colloidal hard-sphere hcp crystal and the effects of epitaxial mismatch on crystal structure, *Phys. Rev. E* **69**, 051602 (2004).
- [21] T. Dasgupta, J. R. Edison, and M. Dijkstra, Growth of defect-free colloidal hard-sphere crystals using colloidal epitaxy, *J. Chem. Phys.* **146**, 074903 (2017).
- [22] M. L. Merrick, W. Luo, and K. A. Fichthorn, Substrate-mediated interactions on solid surfaces: theory, experiment, and consequences for thin-film morphology, *Prog. Surf. Sci.* **72**, 117 (2003).
- [23] C. Ratsch, A. P. Seitsonen, and M. Scheffler, Strain dependence of surface diffusion: Ag on Ag(111) and Pt(111), *Phys. Rev. B* **55**, 6750 (1997).
- [24] A. M. Stoneham, Elastic interactions between surface adatoms and between surface clusters, *Solid State Commun.* **24**, 425 (1977).
- [25] S. Bommel, N. Kleppmann, C. Weber, H. Spranger, P. Schäfer, J. Novak, S. V. Roth, F. Schreiber, S. H. L. Klapp, and S. Kowarik, Unravelling the multilayer growth of the fullerene C<sub>60</sub> in real time, *Nat. Commun.* **5**, 5388 (2014).
- [26] M. Mondal, C. K. Mishra, R. Banerjee, S. Narasimhan, A. K. Sood, and R. Ganapathy, Cooperative particle rearrangements facilitate the self-organized growth of colloidal crystal arrays on strain-relief patterns, *Sci. Adv.* **6**, eaay8418 (2020).
- [27] H. Brune, M. Giovannini, K. Bromann, and K. Kern, Self-organized growth of nanostructure arrays on strain-relief patterns, *Nature (London)* **394**, 451 (1998).

- [28] V. A. Shchukin and D. Bimberg, Spontaneous ordering of nanostructures on crystal surfaces, *Rev. Mod. Phys.* **71**, 1125 (1999).
- [29] J. V. Barth, G. Costantini, and K. Kern, Engineering atomic and molecular nanostructures at surfaces, *Nature (London)* **437**, 671 (2005).
- [30] V. J. Anderson and H. N. Lekkerkerker, Insights into phase transition kinetics from colloid science, *Nature (London)* **416**, 811815 (2002).
- [31] See Supplemental Material at <http://link.aps.org/supplemental/10.1103/PhysRevLett.129.088003>, which includes Refs. [32–41], for additional information on materials and methods, results, and videos.
- [32] Y. Xia, E. Kim, X. M. Zhao, J. A. Rogers, M. Prentiss, and G. M. Whitesides, Complex optical surfaces formed by replica molding against elastomeric masters, *Science* **273**, 347 (1996).
- [33] Keng-hui Lin, John C. Crocker, Vikram Prasad, Andrew Schofield, D. A. Weitz, T. C. Lubensky, and A. G. Yodh, Entropically Driven Colloidal Crystallization on Patterned Surfaces, *Phys. Rev. Lett.* **85**, 1770 (2000).
- [34] J. C. Crocker and D. G. Grier, Methods of digital video microscopy for colloidal studies, *J. Colloid Interface Sci.* **179**, 298 (1996).
- [35] J. R. Savage, D. W. Blair, A. J. Levine, R. A. Guyer, and A. D. Dinsmore, Imaging the sublimation dynamics of colloidal crystallites, *Science* **314**, 795 (2006).
- [36] C. K. Mishra, A. Rangarajan, and R. Ganapathy, Two-Step Glass Transition Induced by Attractive Interactions in Quasi-Two-Dimensional Suspensions of Ellipsoidal Particles, *Phys. Rev. Lett.* **110**, 188301 (2013).
- [37] S. Sacanna, W. T. M. Irvine, P. M. Chaikin, and D. J. Pine, Lock and key colloids, *Nature (London)* **464**, 575 (2010).
- [38] Jacob N. Israelachvili, *Intermolecular and Surface Forces* (Academic Press, New York, 2011).
- [39] Z. Wang, A. M. Alsayed, A. G. Yodh, and Y. Han, Two-dimensional freezing criteria for crystallizing colloidal monolayers, *J. Chem. Phys.* **132**, 154501 (2010).
- [40] Z. Wang, F. Wang, Y. Peng, Z. Zheng, and Y. Han, Imaging the homogeneous nucleation during the melting of superheated colloidal crystals, *Science* **338**, 87 (2012).
- [41] Y. Mao, M. E. Cates, and H. N. W. Lekkerkerker, Depletion force in colloidal systems, *Physica (Amsterdam)* **222A**, 10 (1995).
- [42] C. K. Mishra, A. K. Sood, and R. Ganapathy, Site-specific colloidal crystal nucleation by template-enhanced particle transport, *Proc. Natl Acad. Sci. U.S.A.* **113**, 12094 (2016).
- [43] I. Daruka and A. L. Barabási, Dislocation-Free Island Formation in Heteroepitaxial Growth: A Study at Equilibrium, *Phys. Rev. Lett.* **79**, 3708 (1997).
- [44] S. L. Hellstrom, Y. Kim, J. S. Fakonias, A. J. Senesi, R. J. Macfarlane, C. A. Mirkin, and H. A. Atwater, Epitaxial growth of DNA-assembled nanoparticle superlattices on patterned substrates, *Nano Lett.* **13**, 6084 (2013).
- [45] Y. Tu and J. Tersoff, Origin of Apparent Critical Thickness for Island Formation in Heteroepitaxy, *Phys. Rev. Lett.* **93**, 216101 (2004).
- [46] G. Meng, J. Paulose, D. R. Nelson, and V. N. Manoharan, Elastic instability of a crystal growing on a curved surface, *Science* **343**, 634 (2014).
- [47] J. R. Savage, S. F. Hopp, R. Ganapathy, S. J. Gerbode, A. Heuer, and I. Cohen, Entropy-driven crystal formation on highly strained substrates, *Proc. Natl. Acad. Sci. U.S.A.* **110**, 9301 (2013).
- [48] A. Ohtake, T. Mano, and Y. Sakuma, Strain relaxation in InAs heteroepitaxy on lattice-mismatched substrates, *Sci. Rep.* **10**, 4606 (2020).
- [49] U. Kürpick, A. Kara, and T. S. Rahman, Role of Lattice Vibrations in Adatom Diffusion, *Phys. Rev. Lett.* **78**, 1086 (1997).
- [50] Y. W. Mo and M. G. Lagally, Anisotropy in surface migration of Si and Ge on Si (001), *Surf. Sci.* **248**, 313 (1991).
- [51] H. Brune, Microscopic view of epitaxial metal growth: Nucleation and aggregation, *Surf. Sci. Rep.* **31**, 125 (1998).
- [52] K. A. Fichtorn and M. Scheffler, Island Nucleation in Thin-Film Epitaxy: A First-Principles Investigation, *Phys. Rev. Lett.* **84**, 5371 (2000).
- [53] S. Ovesson, A. Bogicevic, G. Wahnström, and B. I. Lundqvist, Neglected adsorbate interactions behind diffusion prefactor anomalies on metals, *Phys. Rev. B* **64**, 125423 (2001).
- [54] J. W. Evans, P. A. Thiel, and M. C. Bartelt, Morphological evolution during epitaxial thin film growth: Formation of 2D islands and 3D mounds, *Surf. Sci. Rep.* **61**, 1 (2006).
- [55] A. Khorshidi, J. Violet, J. Hashemi, and A. A. Peterson, How strain can break the scaling relations of catalysis, *Nat. Catal.* **1**, 263 (2018).
- [56] S. Arai and H. Tanaka, Surface-assisted single-crystal formation of charged colloids, *Nat. Phys.* **13**, 503 (2017).